Monte Carlo Study of a Three-Dimensional Semi-infinite Spin-1/2 System Limited by a Spin-1 Surface

O. Elgarraoui[a], K. El Kihel[a], M. Monkade[a], M. Madani[b] and M. El Bouziani[a,*]

[a] *Theoretical Physics Group, LPMC Laboratory, Faculty of Sciences, Chouaïb Doukkali University, 24000 El Jadida, Morocco*
[b] *Department of Physics-Chemistry, CRMEF, Meknes, Morocco*

Received: 06.09.2023 & Accepted: 18.01.2024

Doi: 10.12693/APhysPolA.145.186 *e-mail: elbouziani.m@ucd.ac.ma

We investigated a three-dimensional semi-infinite spin-1/2 system bounded by a spin-1 surface using a Monte Carlo simulation based on the Metropolis algorithm. The exchange interactions and crystal field effects on phase diagrams, magnetizations, and susceptibilities were investigated. The phase diagrams in three planes were presented due to the competition between specific system parameters. The system demonstrated ordinary, extraordinary, surface, and special second-order phase transitions, as well as a surface first-order phase transition. Furthermore, tricritical and critical end-points were discovered.

topics: surface transitions, semi-infinite, Ising model, Monte Carlo simulation

1. Introduction

The magnetic properties of semi-infinite systems bound in one direction by a free surface have received increasing attention in the recent decade. The surface effect has a major influence on magnetic features; the surface disrupts a system's translation symmetry and modifies local values [1, 2]. In addition, due to their surprising physical features and wide range of applications, semi-infinite systems have sparked a lot of interest in the statistical physics of phase transitions [3–5].

Some critical characteristics of a semi-infinite system have been investigated experimentally. The surface ordered at a temperature above the bulk in Gd [6] and Co/Ni (111) overlayers [7] is detected via electron-capture spectroscopy and surface-dedicated first-principles techniques; the transitions are surface and extraordinary, respectively. Furthermore, spin-polarized secondary electron emission spectroscopy and the magneto–optic Kerr effect are utilized to demonstrate that the surface and bulk magnetizations of a Gd ferromagnet transit at the same critical temperature, indicating that the ordinary phase transition occurs [8]. The full-potential linearized augmented plane-wave application of correlated band theory, on the other hand, is employed to increase the critical temperature at the surface of Gd(0001) [9].

Numerous theoretical techniques have been used to examine the magnetic characteristics of semi-infinite systems to explain the phenomena seen in experiments. Mean-field approximation (MFA) [10, 11], Monte Carlo simulation (MCS) [12, 13], renormalization group theory (RGT) [14, 15], effective-field theory (EFT) [16], finite cluster approximation [17], Landau theory [18], and series expansions [19] have all been used to investigate the spin-$\frac{1}{2}$ semi-infinite Ising model. Most of these works describe four different forms of second-order phase transitions based on the ratio $R = J_B/J_S$ of bulk and surface interactions: ordinary, extraordinary, surface, and special phase transitions. This system also displays the tricritical, multicritical, and tetracritical points. However, the exact solution of this system is examined and reveals simply the presence of the ordinary second-order phase transition [20, 21].

Later, much attention has been accorded to semi-infinite systems with spin greater than $\frac{1}{2}$, such as the semi-infinite spin-1 and spin-$\frac{3}{2}$ Ising models, which have been explored using numerous approaches, including MFA [22–24] and RGT [25, 26]. Furthermore, because of their distinctive and unexpected characteristics compared to single-spin Ising systems, mixed-spin Ising systems have been effectively employed to explore the magnetic characteristics of ferrimagnetic materials [27]. From

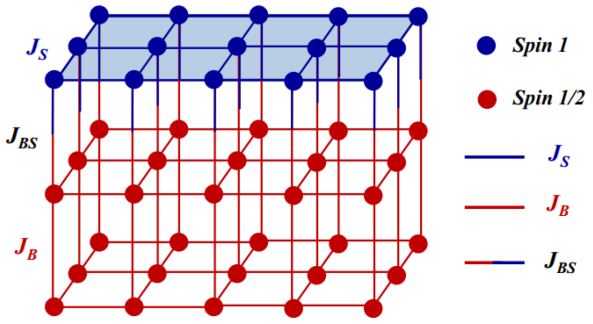

Fig. 1. Schematic representation of a three-dimensional semi-infinite spin-$\frac{1}{2}$ system limited by the free surface occupied by spin-1.

a theoretical standpoint, critical behaviors of the semi-infinite systems with mixed spins $(\frac{1}{2}, \frac{3}{2})$, $(\frac{1}{2}, \frac{5}{2})$, and $(1, \frac{3}{2})$ have been widely investigated using various approaches such as MFA and MCS [28] and RGT [29–31].

However, the study of semi-infinite systems limited by a different spin surface has attracted growing interest in the study of magnetic thin films because of their technological applications, including contemporary data storage [32]. Spintronic systems' technology may be readily controlled and modified in numerous ways, allowing for a wide range of functionality based on their inherent memory and intrinsically complex multiform behavior [33]. Thus, spintronics has been applied to the creation of information storage and advancing sensor technology (extremely high sensitivity, reduced size), as well as in the field of medicine and therapy based on magnetic resonance imaging (MRI) [34]. Studies on hydrogen concentration measurement using ferromagnetic resonance (FMR) in hydrogen gas sensors [35, 36] are employed in different industries, such as chemical, energy, and automotive, and even in residential and industrial applications to assure safety and in the space industry. Furthermore, this type of system has been investigated in other papers, such as [37], which investigated the spin-$\frac{1}{2}$ semi-infinite system bounded by a spin-1 surface in a dynamic situation using mean-field approximation (MFA). In addition, in [38], the authors have investigated the spin-$\frac{1}{2}$ semi-infinite system restricted by the spin-$\frac{3}{2}$ surface, as well as the spin-$\frac{3}{2}$ semi-infinite system bounded by the spin-$\frac{1}{2}$ surface, using the renormalization group theory (RGT) and Monte Carlo simulation (MCS).

More specifically, Kaneyoshi [39] investigated the temperature dependences of surface and bulk magnetizations of a semi-infinite simple cubic mixed spin $(\frac{1}{2}, 1)$ ferromagnetic Ising alloy with a $(1, 0, 0)$ surface within the framework of effective field theory with correlation. They determined a critical value of the crystal field at which the system exhibits a specific type of phase diagram. We also cite the work of Benayad and Zittartz [40], who used RGT to investigate the effects of bilinear and biquadratic interactions on the surface behaviors of the three-dimensional semi-infinite mixed spin-$\frac{1}{2}$ and spin-1 Ising model. They found ordinary, extraordinary, surface, and special phase transitions, as well as 26 fixed points. Recently, Sabri et al. [37] investigated the kinetic phase transition in the semi-infinite mixed spin $(\frac{1}{2}, 1)$ Ising model using the Glauber-type stochastic dynamics method; the system exhibits ordinary, extraordinary, surface, and special phase transitions of second-order and tricritical phenomenon points.

The goal of this study is to investigate the critical behaviors of a three-dimensional semi-infinite spin-$\frac{1}{2}$ system limited by the free surface spin-1 using Monte Carlo simulation. Our research focuses on the effects of reduced exchange interactions and reduced crystal field on phase diagrams, sublattice magnetizations, and susceptibilities. All phases in the bulk and on the surface are determined, including ordinary, extraordinary, surface, and special phase transitions. The model and the Monte Carlo simulation are given in Sect. 2. The effects of the ratios R_B, R_{BS}, and D_S on the phase diagrams, magnetizations, and susceptibilities are investigated in Sect. 3, and the findings are presented in Sect. 4.

2. Model and Monte Carlo simulation

An example of a simple cubic semi-infinite spin-$\frac{1}{2}$ system limited by a spin-1 surface is schematized in Fig. 1. Our system's Hamiltonian is expressed as

$$\beta H = -J_S \sum\nolimits_{\langle i,j \rangle} S_i S_j - J_B \sum\nolimits_{\langle k,l \rangle} \sigma_k \sigma_l - J_{BS} \sum\nolimits_{\langle i,k \rangle} S_i \sigma_k - \Delta_S \sum\nolimits_i S_i^2, \quad (1)$$

where $S = \pm 1, 0$ and $\sigma = \pm 1/2$ indicate the surface and bulk sublattice spin variables, respectively. A ferromagnetic interactions J_S (> 0) and J_B (> 0) connect the two nearest-neighbor spins of surface and bulk, respectively, $\langle i, j \rangle$ and $\langle l, k \rangle$. Next, J_{BS} (< 0) is the exchange interaction between bulk and surface spins, and Δ_S is the surface sublattice crystal field.

To simulate our Hamiltonian stated above in (1), we used Monte Carlo simulation based on the Metropolis algorithm [41]. Periodic boundary conditions are imposed in the XY plane with $N = 30$ spins along the x and y axes, or free boundary conditions are enforced in the z direction, with $L = 31$ being the system length. In this simulation, we flipped the spin once and obtained simulation data with 10^5 MCS, after which the first 10^4 steps were eliminated to equilibrate the system. Our program computes the physical quantities listed below

$$m_S = \frac{1}{N_S} \sum\nolimits_{i=1}^{N_S} S_i, \quad m_B = \frac{1}{N_B} \sum\nolimits_{k=1}^{N_B} \sigma_k. \quad (2)$$

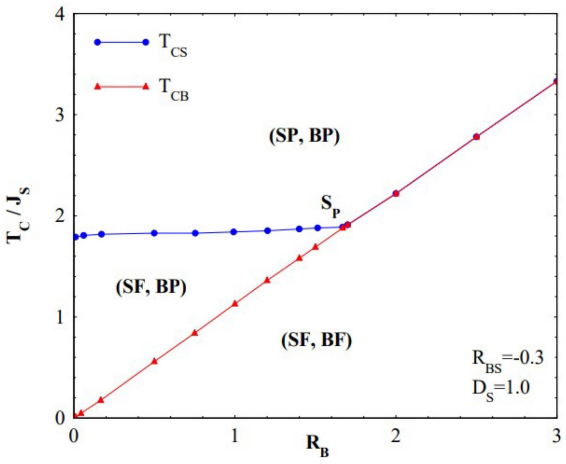

Fig. 2. Phases diagram of the system in the $(T_C/J_S,\ R_B)$ plane evaluated for $R_{BS} = -0.3$ and $D_S = 1.0$; S_P denotes the special point.

The total susceptibility per site of the surface and the bulk is defined by

$$\chi_S = \beta N_S \left(\langle m_S^2\rangle - \langle m_S\rangle^2\right),$$
$$\chi_B = \beta N_B \left(\langle m_B^2\rangle - \langle m_B\rangle^2\right), \quad (3)$$

where $N_S = N \times N$ and $N_B = N \times N \times (L-1)$ indicate the number of surface and bulk spins, respectively, and $\beta = (k_{\rm B}T)^{-1}$, with $k_{\rm B}$ representing the Boltzmann constant and T — absolute temperature. For the sake of simplicity, we set $k_{\rm B} = 1$. The transition temperature T_C is calculated in this study using the divergence of the susceptibility curves.

3. Results and discussions

In this section, we will discuss the effects of the exchange interaction $(J_B,\ J_{BS})$ and single-ion anisotropy Δ_S on the magnetizations, the magnetic susceptibility, and the phase diagrams of the three-dimensional semi-infinite system limited by a free surface. In this study, for simplicity, we use the notation $R_B = J_B/J_S$, $R_{BS} = J_{BS}/J_S$, and $D_S = \Delta_S/J_S$, such that R_B, R_{BS}, and D_S are dimensionless. In addition, we take $J_S = 1$ as the unit of the system. Some interesting results are presented in Figs. 2–7.

It is best to describe the following phases before going to the phase diagrams:

- (SF, BF): both the surface and the bulk are ferromagnetic.
- (SF, BP): the surface is ferromagnetic, while the bulk is paramagnetic.
- (SP, BP): the surface is paramagnetic, as is the bulk.
- (SF_0, BF): the surface is ferromagnetic with spin state $S = 0$ and the bulk is ferromagnetic.

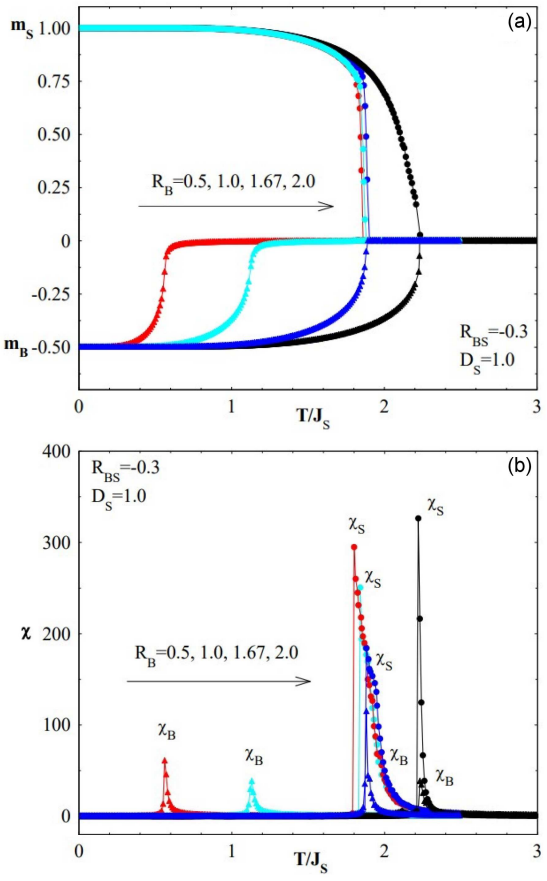

Fig. 3. Reduced temperature dependence of (a) the magnetizations $(m_S,\ m_B)$ and (b) the magnetic susceptibilities (χ_S, χ_B) with $R_{BS} = -0.3$ and $D_S = 1$, and for selected values of R_B ($R_B = 0.5$, 1.0, 1.67, 2.0).

- (SF_1, BF): the surface is ferromagnetic with spin state $S = 1$ and the bulk is ferromagnetic.
- (SF_1, BP): the surface is ferromagnetic with spin state $S = 1$ and the bulk is paramagnetic.

3.1. Effect of the reduced exchange interaction of the bulk (R_B)

Figure 2 depicts the surface and bulk critical temperatures , T_{CS} and T_{CB}, as functions of R_B, with fixed values $R_{BS} = -0.3$ and $D_S = 1.0$. According to this figure and the values of the ratios R_B, the phase diagram shows four types of second-order phase transitions: ordinary, extraordinary, surface, and special. For $R_B < 1.67$ and increasing temperature, our system undergoes extraordinary and surface second-order phase transitions, separating the three phases, namely (SF, BF), (SF, BP), and (SP, BP). However, if $R_B > 1.67$, the corresponding phase diagram shows an ordinary phase transition; the system goes from (BF, SF) to

(SP, BP). However, when $R_B = 1.67$, the surface and bulk of our semi-infinite system become ordered simultaneously ($T_{CS} = T_{CB}$), resulting in a special second-order phase transition at S_P $(1.88, 1.67)$. Similar phase diagrams have been shown in three-dimensional semi-infinite mixed spins $(\frac{1}{2}, 1)$ within the RGT [40], and they have also been seen in the investigation of the kinetic semi-infinite spin-$\frac{1}{2}$ Ising model with an oscillating field [42]. To validate these findings, we investigated the temperature dependence of magnetization and susceptibility, as shown in Fig. 3a, b.

The surface and bulk magnetization curves (m_S and m_B), as well as the surface and bulk susceptibility peaks (χ_S and χ_B) vs reduced temperature (T/J_S) for chosen values of $R_B = 0.5$, 1.0, 1.67, 2.0, with $R_{BS} = -0.3$ and $D_S = 1.0$, are shown in Fig. 3a and Fig. 3b, respectively. At zero temperature, the bulk and surface magnetizations are -0.5 and 1.0, respectively, as illustrated in Fig. 3a. When $R_B < 1.67$, the bulk magnetization grows monotonically to zero at the transition temperature $T_{CB} = 0.56$ as for $R_B = 0.5$; hence, an extraordinary second-order phase transition occurs, separating the (SF, BF) and (SF, BP) phases. The surface magnetization gradually declines until it disappears above the critical temperature $T_{CS} = 1.83$ as for $R_B = 1.0$, indicating a surface second-order phase transition between the (SF, BP) and (SP, BP) phases. The linear variation in temperature of surface magnetization has been seen in numerous semi-infinite crystalline magnets in experiments [43]. If $R_B = 1.67$, the surface and bulk magnetization curves disappear continuously at a particular critical temperature $T_{CS} = T_{CB} = 1.88$, indicating the occurrence of a special phase transition. Above this last particular point, and as the temperature increases, the surface and bulk magnetizations remain constant at the same critical temperature, i.e., $T_{CS} = T_{CB} = 2.23$ as for $R_B = 2.0$; the transition is ordinary of second-order between two phases — (SF, BF) and (SP, BP). Figure 3b depicts the temperature fluctuations of the surface and bulk susceptibilities. We see that for all R_B values chosen, the curves of surface and bulk susceptibilities show a sudden rise at surface and bulk critical temperatures, subsequently accompanied by a decrease. This is a singular behavior, indicating that the system shows a second-order transition. A similar phenomenon has been seen in [40].

3.2. Effect of the reduced exchange interaction between the bulk and the surface (R_{BS})

We also examine the effect of the reduced exchange interaction between the bulk and the surface, R_{BS}, on the surface and bulk critical temperatures, T_{CS} and T_{CB}. Therefore, we plotted the phase diagram in the $(T_C/J_S, R_{BS})$ plane for a fixed value of $R_B = 0.5$ and $D_S = 1.0$ in Fig. 4. The

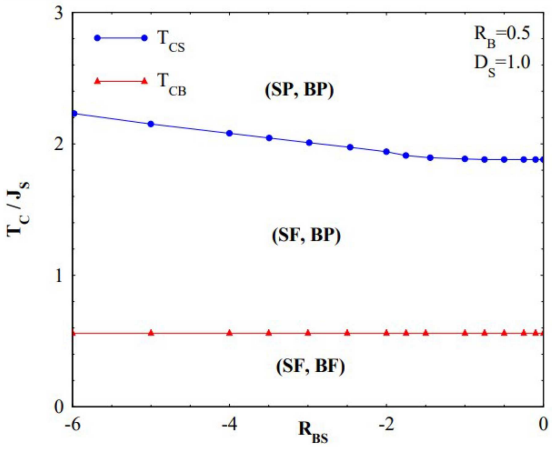

Fig. 4. Phases diagram of the system in the $(T_C/J_S,\ R_{BS})$ plane evaluated for $R_B = 0.5$ and $D_S = 1.0$.

phase diagram shows two second-order phase transition lines for all negative R_{BS} values, dividing three phases. When the system transits from the (SF, BF) phase to the (SF, BP) phase at $T_{CB} = 0.57$, this is called an extraordinary phase transition. The surface phase transition line remains constant ($T_{CS} = 1.90$) for $R_{BS} > -1.57$ and climbs with a little slope as R_{BS} decreases, between (SF, BP) and (SF, BP) phases at higher temperatures. The critical behaviors are qualitatively comparable to those observed in the kinetic semi-infinite spin-$\frac{1}{2}$ Ising model using MFA [42], in a ferrimagnetic mixed-spin $(\frac{1}{2}, 1)$ Ising double layer superlattice [44], and in a multilayer system [45] using MCS.

To further understand the critical behaviors of our semi-infinite system, i.e., the phase diagrams presented above, we will show the temperature dependences of the surface and bulk magnetizations (m_S and m_B) and magnetic susceptibilities (χ_S and χ_B) with $R_B = 0.5$ and $D_S = 1.0$, as well as for chosen values of R_{BS} ($R_{BS} = -0.1$, -1.5, -3.5) in Fig. 5a, b. According to Fig. 5a, for all negative R_{BS} values, the bulk magnetization has a saturation value of $m_B = -0.5$ at $T = 0$ K and vanishes beyond a critical temperature ($T_{CB} = 0.57$); the system exhibits an extraordinary second-order phase transition. Surface magnetization mS, on the other hand, drops continuously to zero at transition temperature (as $T_{CS} = 1.90$, 2.05 for $R_{BS} = -0.1$, -3.5, respectively) as a result of a surface phase transition. Furthermore, the thermal variation of the susceptibilities (χ_S and χ_B) may be used to calculate the surface and bulk critical temperatures, as shown in Fig. 5b. We can see that the surface and bulk susceptibilities increase rapidly as temperature increases, reaching their maximums at T_{CB} and T_{CS}, respectively. All of these peaks represent extraordinary and surface second-order phase transitions. A similar phase diagram has been found in [45] using Monte Carlo simulation (MCS).

3.3. Effect of the reduced crystal field (D_S)

Finally, the phase diagram is depicted in the $(T_C/J_S, D_S)$ plane for two cases: One for a fixed value of $R_B = 0.3$ and $R_{BS} = -0.3$, and the other for $R_B = 1.0$ and $R_{BS} = -0.3$, as shown in Figs. 6 and 7.

3.3.1. For $R_B = 0.3$ and $R_{BS} = -0.3$

The phase diagram in Fig. 6a illustrates the surface and extraordinary second-order phase transitions, as well as the surface first-order phase transition and tricritical point (T^*). The surface of the system transits from the (SF_0, BF) phase to the (SF_1, BF) phase at lower temperatures and when D_S rises — this is the first-order phase transition (dashed line). In addition, the corresponding phase diagram shows an extraordinary second-order phase transition (red line) between the (SF, BF) and (SF, BP) phases. Furthermore, our system

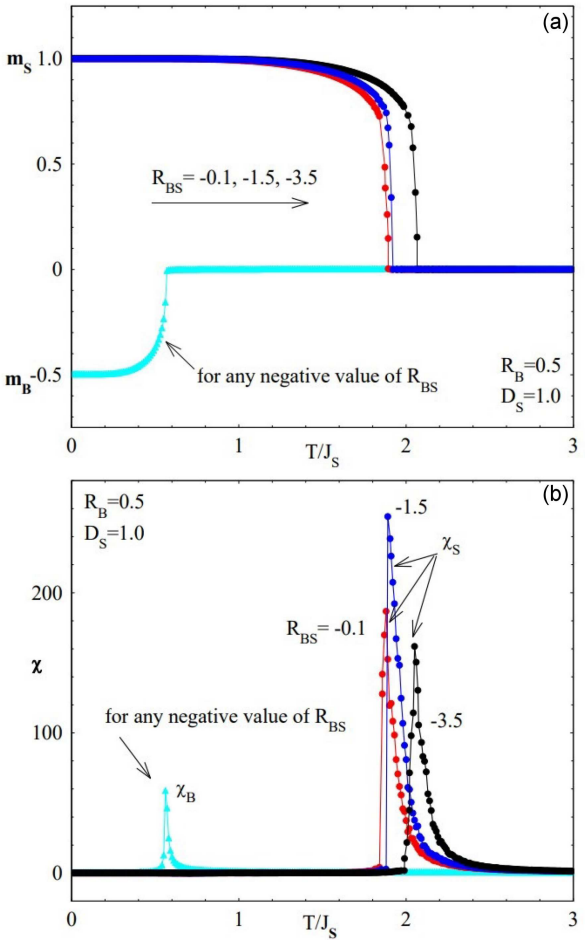

Fig. 5. Reduced temperature dependence of (a) the magnetizations (m_S, m_B) and (b) the magnetic susceptibilities (χ_S, χ_B) with $R_B = 0.5$ and $D_S = 1.0$, and for selected values of R_{BS} ($R_{BS} = -0.1$, -1.5, -3.5).

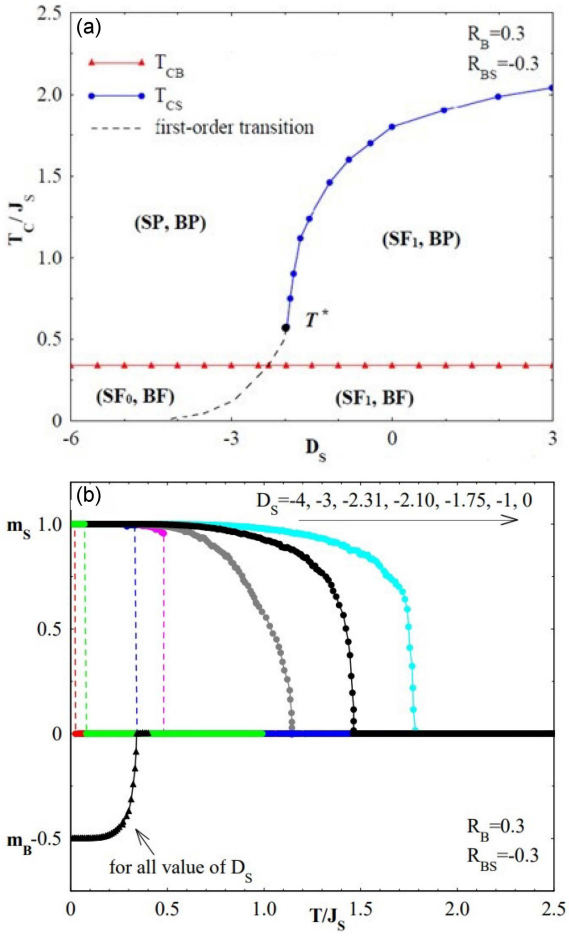

Fig. 6. (a) Phases diagram of the system in the $(T_C/J_S, D_S)$ plane. (b) Reduced temperature dependence of the magnetizations (m_S, m_B) evaluated for $R_B = 0.3$ and $R_{BS} = -0.3$; T^* denotes the corresponding tricritical point.

shows a surface second-order phase transition that divides two phases, i.e., (SF, BP) and (SP, BP). By raising the temperature, our system displays the tricritical point T^* with coordinates $(-1.97, 0.57)$, where the surface first-order phase transition line changes to a surface second-order one. To verify the nature (continuous or discontinuous) of the phase transition seen in Fig. 6a, we plot the surface and bulk magnetization curves (m_S and m_B) vs temperature in Fig. 6b for the chosen value of D_S ($D_S = -4$, -3, -2.31, -2.10, -1.75, -1, 0). For all values of D_S, the bulk magnetizations are $m_B = -0.5$ at zero temperature and grow to the same critical temperature ($T_{CB} = 0.34$); the bulk of the system undergoes an extraordinary second-order phase transition. Meanwhile, for $D_S < -0.57$ as for $D_S = -3.0$ and -2.31, the surface magnetization discontinuously passes from saturation to zero at $T_t = 0.07$ and 0.345, respectively; the surface of the system exhibits a surface first-order phase transition between ($m_S = 1.0$, $m_B = 1/2$) and ($m_S = 0.0$, $m_B = 1/2$) phases.

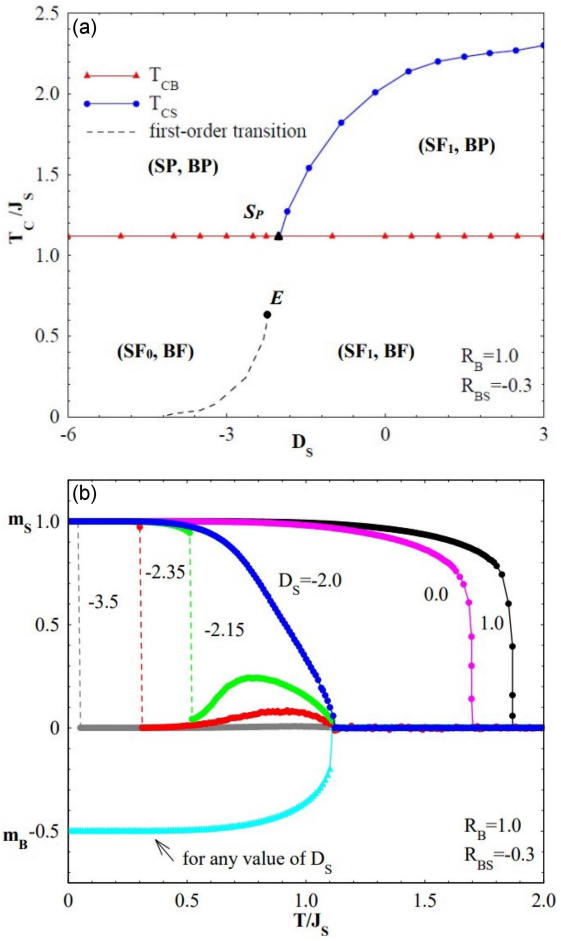

Fig. 7. (a) Phases diagram of the system in the $(T_C/J_S,\ D_S)$ plane. (b) Reduced temperature dependence of the magnetizations (m_S, m_B) evaluated for $R_B = 1$ and $R_{BS} = -0.3$; S_P and E denote the corresponding special and critical end-points, respectively.

However, when $D_S > -0.57$, the magnetization m_S diminishes continuously to the critical temperature $T_{CS} = 1.16$ as for $D_S = -1.75$. Hence, a second-order surface phase transition occurs. Several three-dimensional semi-infinite systems using various theories, such as MFA and RGT, show similar results [24, 25, 37, 42].

3.3.2. For $R_B = 1.0$ and $R_{BS} = -0.3$

As a final point, we show in Fig. 7a the critical behaviors T_C/J_S as a function of D_S for $R_{BS} = -0.3$ and $R_B = 1.0$. The phase transitions shown in this figure are the first-order and second-order phase transitions. The free surface undergoes a first-order transition between two ordered phases, i.e., (SF_0, BF) and (SF_1, BF), at lower temperatures. This transition line terminates at the critical end-point E with coordinates $(-2.11, 0.66)$, and smooth continuity occurs between these phases after this E point. The system displays an extraordinary second-order phase transition at critical temperature $T_{CB} = 1.12$ for all values of D_S; the transition is from the (SF, BF) phase to the (SP, BP) phase. The bulk and surface of our semi-infinite system are ordered at the same critical temperature $T_{CB} = T_{CS}$ at the special point located at S_P $(-2.0, 1.12)$; the special second-order phase transition occurs. Our system shows the surface second-order phase transition above this particular point, which divides two phases, namely (SF, BP) and (SP, BP). To confirm these phase transitions, we studied the temperature variation of the surface and bulk magnetizations for various values of D_S ($D_S = -3.5$, -2.35, -2.15, -2.0, 0.0, 1.0) with $R_{BS} = -0.3$ and $R_B = 1.0$ in Fig. 7b. This figure clearly shows that when T/J_S grows, the bulk magnetizations continuously fall to zero at the same critical temperature for all specified values of D_S. The bulk of the system exhibits extraordinary phase transition, whereas the surface of the system exhibits a first-order phase transition for all values of $D_S < -2.11$, since the surface magnetization exhibits a discontinuous leap from ($m_S = 1$, $m_B = 1/2$) phase to ($m_S = 0$, $m_B = 1/2$) at $T_t = 0.31$ as for $D_S = -2.35$. When $D_S = -2.0$, the bulk and surface are ordered concurrently at $T_{CB} = T_{CS} = 1.12$. When $D_S > -2.0$, the (SF, BP)–(SP, BP) transition is a second-order surface phase transition. Similar findings have been obtained in numerous semi-infinite systems studied within the framework of the EFT and the cluster variation approximation [46–48]. Also, this type of phase diagram has been found using RGT and MCS [38]. However, no intuitively specific phase transitions have been detected. This is the case when the critical bulk temperature is higher than the surface temperature, independent of the bulk–surface interaction ratio values, indicating that all bulk phase transitions are remarkable. The critical temperature of the bulk is always lower than that of the surface when the transition is of the second order. These findings are more reliable due to the Monte Carlo simulation (MCS).

4. Conclusions

In this study, we investigated, within the Monte Carlo simulation, the effects of the reduced parameters R_B, R_{BS}, and D_S on the critical behavior of a ferromagnetic three-dimensional semi-infinite spin-$\frac{1}{2}$ system limited by a ferromagnetic spin-1 surface. Phase diagrams were plotted in three different planes after determining the thermal variations of magnetizations and susceptibilities. In the $(T_C/J_S, R_B)$ plane and according to the values of ratios R_B, our semi-infinite system exhibits ordinary, extraordinary, surface, and special second-order phase transitions, while in the plane $(T_C/J_S, R_{BS})$, the system presents only extraordinary and surface second-order transitions. The third $(T_C/J_S, D_S)$ plane illustrates many

interesting results, such as the extraordinary and special phase transitions, the surface second- and first-order phase transitions, and the tricritical and critical end-points.

References

[1] K. Binder, *Critical Behavior at Surfaces, Phase Transitions and Critical Phenomena*, Eds. C. Domb, J.L. Lebowitz, Academic Press, New York 1983, p. 8.

[2] H.W. Diehl, *Int. J. Mod. Phys. B* **11**, 3503 (1997).

[3] C. Rau, C. Jin, M. Robert, *J. Appl. Phys.* **63**, 3667 (1988).

[4] M. Polak, L. Rubinovich, J. Deng, *Phys. Rev. Lett.* **74**, 4059 (1995).

[5] H. Dosch, *Critical Phenomena at Surfaces and Interfaces*, Springer, Berlin 1992.

[6] C. Rau, M. Robert, *Phys. Rev. Lett.* **58**, 2714 (1987).

[7] F. Gimbert, L. Calmels, S. Andrieu, *Phys. Rev. B* **84**, 094432 (2011).

[8] C.S. Arnold, D.P. Pappas, *Phys. Rev. Lett.* **85**, 5202 (2000).

[9] A.B. Shick, W.E. Pickett, C.S. Fadley, *Phys. Rev. B* **61**, 9213 (2000).

[10] A.J. Bray, M.A. Moore, *J. Phys. A Math. Gen.* **10**, 1927 (1977).

[11] M. Saber, *J. Phys. C Solid State Phys.* **20**, 2749 (1987).

[12] K. Binder, D.P. Landau, *Phys. Rev. Lett.* **52**, 318 (1984).

[13] S.V. Belim, E.V. Trushnikova, *Phys. Met. Metallogr.* **119**, 441 (2018).

[14] N.M. Švrakić, R. Pandit, M. Wortis, *Phys. Rev. B* **22**, 1286 (1980).

[15] R. Lipowsky, H. Wagner, *Z. Phys. B Condens. Matter* **42**, 355 (1981).

[16] T. Kaneyoshi, I. Tamura, E.F. Sarmento, *Phys. Rev. B* **28**, 6491 (1983).

[17] A. Benyoussef, N. Boccara, M. Saber, *J. Phys. C* **18**, 4275 (1985).

[18] R. Lipowsky, W. Speth, *Phys. Rev. B* **28**, 3983 (1983).

[19] K. Binder, P.C. Hohenberg, *Phys. Rev. B* **9**, 2194 (1974).

[20] H. Au-Yang, M.E. Fisher, *Phys. Rev. B* **21**, 3956 (1980).

[21] M.E. Fisher, A.E. Ferdinand, *Phys. Rev. Lett.* **19**, 169 (1967).

[22] A. Benyoussef, N. Boccara, M. Saber, *J. Phys. C Solid State Phys.* **19**, 1983 (1986).

[23] A. Bakchich, M. El Bouziani, *Phys. Rev. B* **56**, 11161 (1997).

[24] A. Bakchich, M. El Bouziani, *J. Phys. Condens. Matt.* **11**, 6147 (1999).

[25] A. Benyoussef, N. Boccara, M. El Bouziani, *Phys. Rev. B* **34**, 7775 (1986).

[26] A. Bakchich, M. El Bouziani, *Phys. Rev. B* **63**, 064408 (2001).

[27] O. Kahn, *Molecular Magnetism*, Courier Dover Publications, 2021.

[28] S. Zouhair, M. Monkade, A. El Antari, M. El Bouziani, N. Hachem, M. Madani, *Surf. Rev. Lett.* **28**, 2150025 (2021).

[29] A. El Antari, A. Alrajhi, M. Bourass, S. Zouhair, M. Madani, N. Hachem, M. El Bouziani, *J. Adv. Phys.* **7**, 281 (2018).

[30] A. El Antari, N. Hachem, A. Al-Rajhi, M. Madani, M. El Bouziani, *Eur. Phys. J. Plus.* **135**, 460 (2020).

[31] M. El Bouziani, M. Madani, A. Gaye, A. Alrajhi, *World J. Condens. Matter Phys.* **6**, 109 (2016).

[32] S.J. Callori, T. Saerbeck, D.L. Cortie, K.-W. Lin, *Solid State Phys.* **71**, 73 (2020).

[33] E.Y. Vedmedenko, R.K. Kawakami, D.D. Sheka, P. Gambardella, A. Kirilyuk, A. Hirohata, C. Binek, O. Chubykalo-Fesenko, S. Sanvito, B.J. Kirby, *J. Phys. D Appl. Phys.* **53**, 453001 (2020).

[34] P.P. Freitas, F.A. Cardoso, V.C. Martins, S.A.M. Martins, J. Loureiro, J. Amaral, C. Fermon, *Lab Chip* **12**, 546 (2012).

[35] C. Lueng, P. Lupo, T. Schefer, P.J. Metaxas, A.O. Adeyeye, M. Kostylev, *Int. J. Hydrogen Energy* **44**, 7715 (2019).

[36] C. Lueng, P. Lupo, P.J. Metaxas, M. Kostylev, A.O. Adeyeye, *Adv. Mater. Technol.* **1**, 1600097 (2016).

[37] S. Sabri, A.G. El Hachimi, M. El Yadari, A. Benyoussef, A. El Kenz, *Physica A* **511**, 207 (2018).

[38] O. Elgarraoui, H. Saadi, M. Monkade, N. Hachem, M. El Bouziani, *Surf. Sci.* **738**, 122369 (2023).

[39] T. Kaneyoshi, *J. Phys. Soc. Jap.* **58**, 1755 (1989).

[40] N. Benayad, J. Zittartz, *Z. Phys. B Condens. Matter* **81**, 107 (1990).

[41] N. Metropolis, A.W. Rosenbluth, M.N. Rosenbluth, A.H. Teller, E. Teller, *J. Chem. Phys.* **21**, 1087 (1953).

[42] A.G. El Hachimi, M. El Yadari, A. Benyoussef, A. El Kenz, L. Bahmad, *Physica A* **410**, 370 (2014).

[43] T. Kaneyoshi, *Introduction to Surface Magnetism*, CRC Press, Boca Raton (FL) 1991.

[44] L.B. Drissi, S. Zriouel, L. Bahmad, *J. Magn. Magn. Mater.* **374**, 639 (2015).

[45] Y.A. Qahoom, R. Aharrouch, K. El Kihel, M. Madani, N. Hachem, M. El Bouziani, *SPIN* **13**, 2340009 (2023).

[46] M. Bentaleb, N. El Aouad, M. Saber, *Phys. Status Solidi B* **231**, 529 (2002).

[47] T. Kaneyoshi, S. Shin, *Physica A* **260**, 455 (1998).

[48] C. Buzano, A. Pelizzola, *Physica A* **216**, 158 (1995).